Optical Engineering

SPIEDigitalLibrary.org/oe

Misfit of rigid tools and interferometer subapertures on off-axis aspheric mirror segments

Ci Song
David Walker
Guoyu Yu

SPIE

Misfit of rigid tools and interferometer subapertures on off-axis aspheric mirror segments

Ci Song
National University of Defense Technology
College of Mechatronic Engineering and Automation
Changsha, Hunan, 410073, China
E-mail: sunicris@163.com

David Walker
University College London
and Zeeko Ltd, National Facility for Ultra-Precision Surfaces
OpTIC-Glyndwr, Ffordd William Morgan
St Asaph Business Park
North Wales, LL17 OJD, United Kingdom
and
Glyndŵr University
OpTIC-Glyndwr, Ffordd William Morgan
St Asaph Business Park
North Wales, LL17 OJD, United Kingdom

Guoyu Yu
Glyndŵr University
OpTIC-Glyndwr, Ffordd William Morgan
St Asaph Business Park
North Wales, LL17 OJD, UK

Abstract. Rigid tools can confer advantages at certain stages of manufacturing off-axis mirror segments, but the misfit due to surface asphericity and asymmetry poses constraints on their application. Types of misfit are classified and, using least squares, the best-fit tool forms with different distances from the pole of the parent asphere are calculated. The outer mirror segment for the European extremely large telescope is taken as a case-study, assuming a rigid tool size of 150 mm. A simple independent approximation validates the calculation. A close parallel is wavefront misfit in subaperture interferometry, which is also considered. [DOI: 10.1117/1.3597328]

Subject terms: misfit; rigid tools; aspheric segment.

Paper 110089RR received Jan. 28, 2011; revised manuscript received May 10, 2011; accepted for publication May 16, 2011; published online Jul. 6, 2011.

1 Introduction

The European extremely large telescope (E-ELT), under development by the European Southern Observatory (ESO) will be 42 m in diameter and will address key science projects such as the era of galaxy-formation and terrestrial extra-solar planets.[1]

The National Facility for Ultraprecision Surfaces, St. Asaph, United Kingdom is producing seven full-size prototype segments for the E-ELT project for ESO. These mirror-segments have an irregular-hexagonal shape to tessellate a curved surface, and an off-axis ellipsoid surface. The nominal segment size is 1.234 m, flat to flat.[1,2] The seven prototype segments form a cluster at the periphery of the 42 m pupil, as shown in Fig. 1.

This paper addresses the potential use of small rigid tools attached to standard rotating polishing bonnets on the Zeeko CNC polishing machine. They can be used to smooth surfaces with loose-abrasive, following diamond-wheel generation of the off-axis asphere. The compression ("Z-offset") of the inflated bonnet provides the tool's contact force.[3–5] The misfit between the tool-surface and the off-axis aspheric surface of the segment limits the maximum tool-size. Empirically, the depth of surface defects caused by such a misfit depend on two main criteria: i. the relationship between misfit and abrasive particle size, and ii. the absolute depth of material removed.

Assuming a raster tool-path, misfit can be managed in two ways:

1. Straight raster-tracks are orientated perpendicular to a line joining the center of the segment to the pole of the primary. The natural wear-rate of the tool is measured on a witness part. Process parameters are chosen so that the tool wear-rate is sufficient for the tool to adapt to the changing asphericity along each raster-track. Tool-wear also changes the *Z*-offset and hence bonnet compression, and the CNC file is modified to compensate.
2. In the special case of an arcuate raster, where the centre of curvature of each arc lies on the axis-of-symmetry of the parent asphere, each raster-track is a a contour of constant asphericity. There is then no change in misfit along each raster-track, although tool-wear must still be compensated in the CNC file.

In either case, the tool is prepared with a rotational aspheric form, chosen to be the best-fit to the local geometry of the segment at the start of the tool-path. Misfit effects then arise from i. the instantaneous change in asphericity on stepping from one raster track to the next, and ii. the rotation of the tool, which forces it to adopt a rotationally-symmetric form despite the cylindrical term in the segment surface.

In this paper, a best-fit of the rotationally-symmetric tool is calculated to investigate the quantitative misfit. An outermost E-ELT segment is simulated: the most severe case. The misfit for given tool sizes and polar distances is

0091-3286/2011/$25.00 © 2011 SPIE

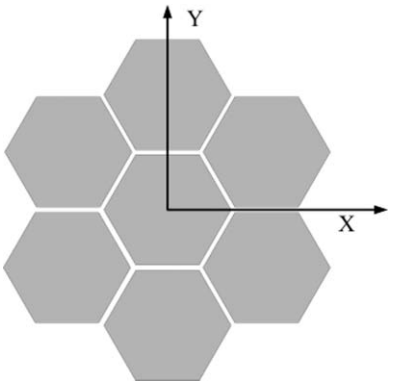

Fig. 1 Prototype segments pattern.

considered in Sec. 4. The analytic simulations are used to compute the tool-misfit on a grid-spacing of 0.1×0.1 mm. The results were then cross-checked using a simple independent method of reduced accuracy and the results used to assess viable maximum tool sizes. Finally, subaperture interferometry is considered, where the wavefront misfit to the best fit spherical wavefront is calculated.

2 Representation of Off-Axis Segment in a Translational and Rotational

2.1 *Reference Frame*

The ELT primary mirror is a conic surface with the following expression:

$$z = \frac{c \cdot \rho^2}{1 + \sqrt{1 - (k+1) \cdot c^2 \cdot \rho^2}}, \tag{1}$$

where$c$ is the curvature of the vertex, k is the conic constant ($k = -e^2$, where e is the eccentricity), and ρ is the distance between point (x, y, z) and original point $(0, 0, 0)$ in the XOYplane ($\rho^2 = x^2 + y^2$). In the ELT project, $c = 1/84{,}000$ mm^{-1} and $k = -0.99, 3295$.

To analyze locally the off-axis section of the conic prototype segment that is centered at the point $(x_0, 0, z_0)$ aligned with the point's normal direction, a new reference frame centered at point $(x_0, 0, z_0)$ should be introduced to describe the conic prototype segment. In addition, some proper translational and rotational relations which will be established between the new reference frame and the original one are described as follows.

$$\begin{aligned} x &= x' \cdot \cos\theta - z' \cdot \sin\theta + x_0 \\ y &= y' \\ z &= x' \cdot \sin\theta + z' \cdot \cos\theta + z_0. \end{aligned} \tag{2}$$

As the parent primary mirror is rotationally-symmetric, the x axis of the original reference can be definitely aligned with the normal direction from point $(0, 0, 0)$ to point $(x_0, 0, z_0)$. It means that two points (x_1, y_1, z_1) and (x_2, y_2, z_2) must attribute the same features in a new local reference frame if they have the same length ($x_1^2 + y_1^2 = x_2^2 + y_2^2 = \rho^2$). In the above equations, the value at point $(x_0, 0, z_0)$ can be expressed as

$$z_0 = \frac{c \cdot x_0^2}{1 + \sqrt{1 - (k+1) \cdot c^2 \cdot x_0^2}}. \tag{3}$$

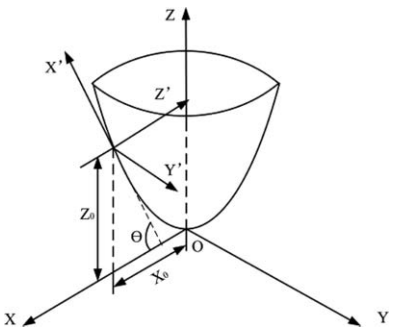

Fig. 2 Local coordinates of the off-axis section centered at the point $(x_0, 0, z_0)$.

Considering that in the new reference frame the z' axis is aligned with the normal direction of conic (shown in Fig. 2), its rotational angle can obtained easily as

$$\tan\theta = z_x, \tag{4}$$

where z_x is the derivative of z with respect to x. With proper geometric transformation and analysis, z_x can be expressed as

$$z_x = \frac{c \cdot x_0}{\sqrt{1 - (k+1) \cdot c^2 \cdot x_0^2}}. \tag{5}$$

With the help of Eqs. (3) and (4), some expressions between point $(x_0, 0, z_0)$ and parameters c, k, and θ can be given by

$$cx_0 = \frac{\sin\theta}{\sqrt{1 + k\sin^2\theta}}, \tag{6}$$

$$1 - (k+1)cz_0 = \frac{\cos\theta}{\sqrt{1 + k\sin^2\theta}}. \tag{7}$$

Substituting Eqs. (2) and (4) into Eq. (1), a conic equation can be obtained in the new reference coordinate system with some algebra transformation.[6,7]

$$z = \frac{t}{b + \sqrt{b^2 - at}}, \tag{8}$$

With the help of

$$\begin{aligned} a &= c(1 + k\cos^2\theta) \\ b &= \frac{1}{\sqrt{1 + k\sin^2\theta}} - ck\sin\theta\cos\theta x \\ t &= c(1 + k\sin^2\theta)x^2 + cy^2. \end{aligned} \tag{9}$$

3 Best-Fit Tool Form Analysis

A fine polishing process requires intimate contact between the lap and the optic, and this naturally occurs when both are spherical with matching radius. However, a misfit also arises when polishing aspherics. To minimize the misfit effect, a best-fit tool should be introduced. The best-fit tool's form is an on-axis conic centered on the portion desired, which can fit the local surface best in the rms sense.

An arcuate tool-path (curved raster) can be configured so that the center of curvature of each track coincides with the vertex of the 42 m primary mirror. In this case, each track is a contour of constant asphericity. During the motion of the tool along the arcuate tool-path (Fig. 3), it continuously wears

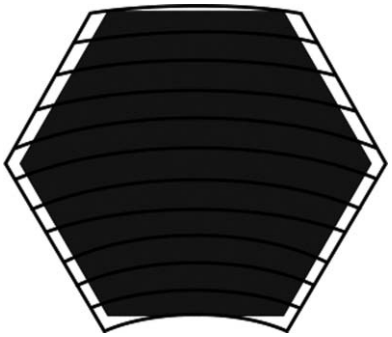

Fig. 3 Arcuate raster tool-path for an off-axis prototype segment (exaggerated curvature).

and the CNC file is configured to allow for the pre-measured wear-rate. The tool's form is a rotationally-symmetric conic and the best-fit to the local segment surface.

Cardona–Nunez et al.[7] have presented a method to approximate an off-axis section by an on-axis conic centered on the portion. Based on a continuum least squares method, an on-axis best-fit conic can be expressed as:

$$z = \frac{c_n \cdot \rho^2}{1 + \sqrt{1 - (k_n + 1) \cdot c_n^2 \cdot \rho^2}}, \tag{10}$$

where c_n is the new curvature of the vertex, and k_n is the conic constant of the on-axis best-fit conic. Their detailed expressions are as follows

$$c_n = 0.5c\delta(1 + \delta^2), \tag{11}$$

$$k_n = [m(1 + 3\delta^2) + n(3 + \delta^2)]/(1 + \delta^2)^3. \tag{12}$$

In addition, the symbol m, n, and δ are defined as

$$m = 4k^2 \sin^2\theta \cos^2\theta + b\delta^2, \tag{13}$$

$$n = 1 + k\cos^2\theta, \tag{14}$$

$$\delta = \sqrt{1 + k\sin^2\theta}. \tag{15}$$

Therefore, a new on-axis conic (in terms of rms) that best fits the off-axis mirror segment can be obtained with Eqs. (11) and (12). Note that the parameters c_n and k_n are independent with the size of the off-axis prototype mirror segment.

For a plausible tool size of 50 mm, the cross section tools with the different polar distances (distance of tool-center from the pole of primary) from 0 to 21 m have been simulated, as shown in Fig. 4(a). The tool's center is defined as the reference point, to accord with the protocol of the Zeeko process. Figure 4(b) shows the variation of edge-heights of tools, for different distances from the pole of the 42 m primary mirror.

4 Principle of Misfit

4.1 *Definition of Misfit*

Fine polishing ideally requires intimate contact between the tool and the optical surface, and this occurs with a spherical optic because of symmetry.[8] However, when a rotating

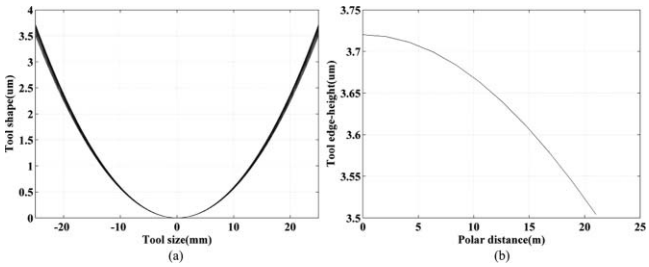

Fig. 4 Best-fit tool rotationally-symmetric form for tool-diameter of 50 mm. (a) Cross section of a 50 mm tool; (b) Tool edge-heights with different polar distances.

(and so rotationally-symmetric) rigid tool moves across an asphere, there is a varying misfit. In the general case of an off-axis asphere (or freeform), where a rotating rigid tool follows a pre-determined tool-path, three types of misfit are defined as:

Misfit-1: Misfit of the rotationally-symmetric rigid tool to the surface

Misfit-2: Misfit due to the change in surface asphericity along one tool-path trajectory.

Misfit-3: The "stepping" misfit between one tool-path trajectory and the next (e.g., between adjacent raster-traverses or spiral-convolutions)

Misfit-1 is effectively the difference between the surface-form over the tool-diameter, and the best-fit rotational-average to the surface-form. In the special case we adopt of the arcuate tool-path, the asphericity is constant along each track, and so Misfit-2 does not arise. For other tool-paths such as a straight raster, it can be managed through tool-wear. Misfit-3 requires quantification, but can be managed through design of the tool-path. When Misfit-3 occurs in the polishing, the total misfit should be obtained with Misfit-3 plus Misfit-1. To evaluate these misfits, a lateral grid spacing of 0.1 mm was used throughout the simulations.

4.2 *Principle of Misfit-1*

To investigate Misfit-1, we adopt the following parameters: the polar distance (distance of tool-center from pole of primary) varies between 1 and 21 m, and four tool sizes with diameter of 50, 100, 150, and 200 mm. The misfit PV is depicted in Fig. 5; as expected, a large tool results in more Misfit-1, and an increased Misfit-1 towards the edge of the pupil.

4.3 *Principle of Misfit-2*

Since Misfit-2 is related with tool-path, two types of raster tool-paths (straight raster and straight cross raster) are investigated in this section, as shown in Fig. 6. Misfit-2 of the straight raster tool-path is the difference between the rotationally-symmetrical best-fitting aspheric to the local surface at point A compared with point B, and Misfit-2 of straight cross raster tool-path is the difference between the rotationally-symmetrical best-fitting aspheric to the local surface at point C compared with point D. Therefore, if the surface is a pure cylindrical form, then Misfit-2 will be zero.

To investigate the relation between Misfit-2, tool-size, and polar distance, the following parameters are adopted: the polar distance (distance of tool-center from pole of primary) varies between 1 and 21 m, and four tool sizes with diameter of 50, 100, 150, and 200 mm. Misfit-2 with straight

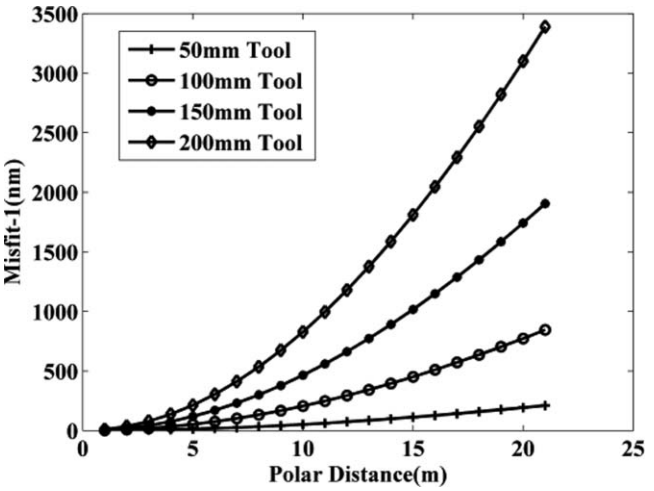

Fig. 5 Relation between Misfit-1 (*p*-to-*v*), tool-size, and polar distance.

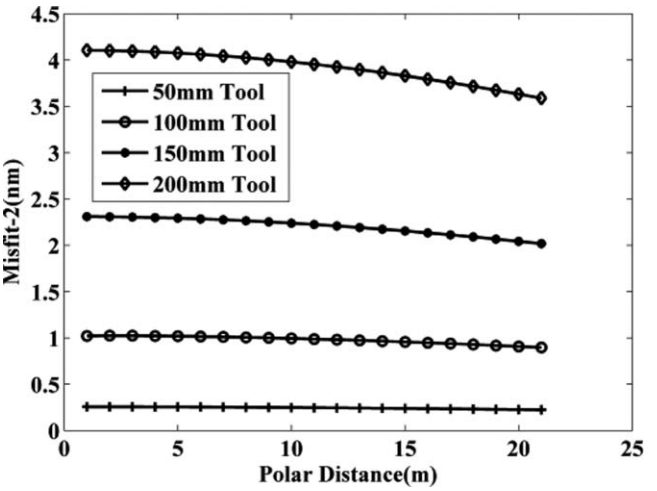

Fig. 7 Relation between Misfit-2 (*p*-to-*v*), tool-size, and polar distance with a straight raster tool-path.

raster tool-path and straight cross raster tool-path are depicted in Figs. 7 and 8, respectively.

4.4 *Principle of Misfit-3*

To investigate the principle of Misfit-3, the polar distance is 21 m, four tool sizes with diameter of 50, 100, 150, and 200 mm are adopted, and the step-size is in the range of 1 to 20 mm. The results are shown in Fig. 9, and show a linear relation between Misfit-3 and the step-size.

5 Quantitative Misfit of the Outermost Off-Axis Mirror Segment for E-ELT

The misfit of an outermost off-axis E-ELT segment constitutes the worst case. As an illustration, $\phi 150\,mm$ tool is evaluated, 21 m from the primary vertex, with a step-size of 10 mm. With the straight raster tool-path, Misfit-2 is almost negligible, as shown in Fig. 7. To observe the distribution of Misfit-1 and Misfit-3, they are simulated. The results of Misfit-1 are shown in Figs. 10(a) and 10(b), showing a saddle form with PV of 19.1 μm Being different from Misfit-1, Misfit-3 is rotationally-symmetrical, as shown in Figs. 11(a) and 11(b). Its PV is 0.17 μm, which is an order of magnitude less than Misfit-1.

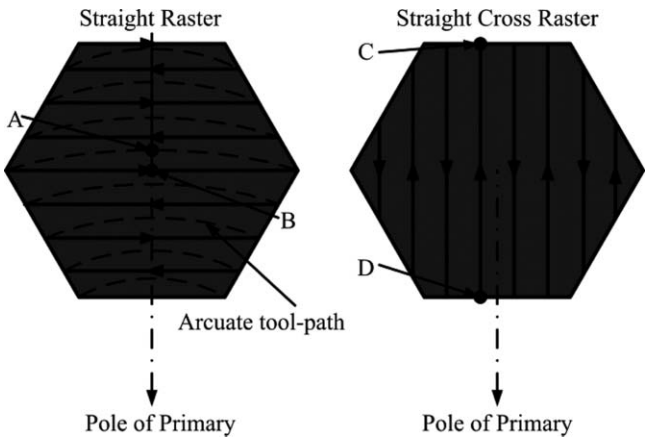

Fig. 6 Two raster tool-path defined in off-axis segment.

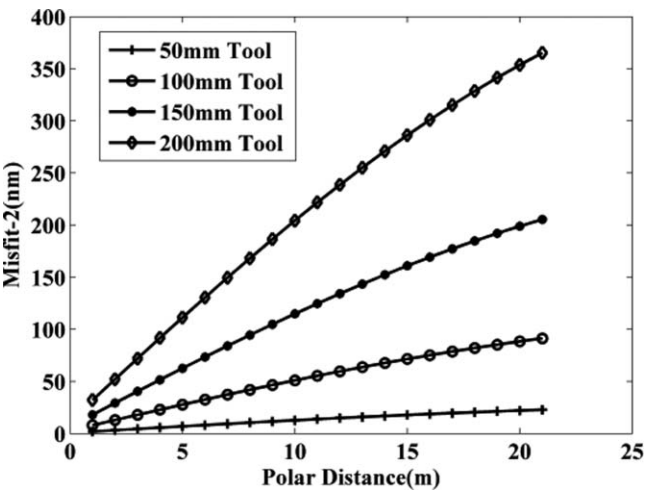

Fig. 8 Relation between Misfit-2 (*p*-to-*v*), tool-size, and polar distance with a straight cross raster tool-path.

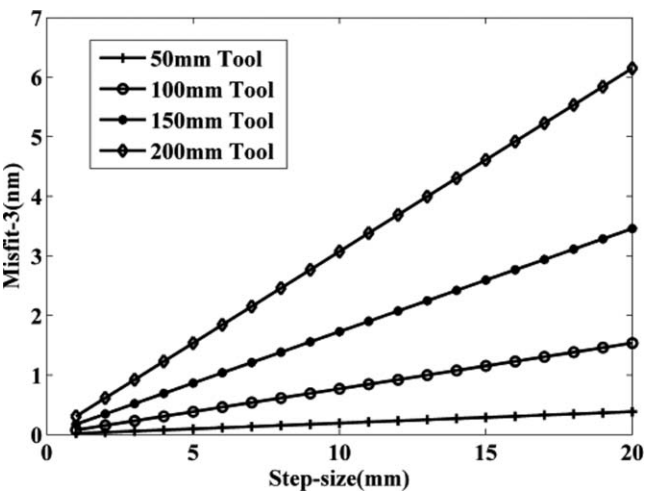

Fig. 9 Relation between Misfit-3 (*p*-to-*v*), tool-size, and step-size.

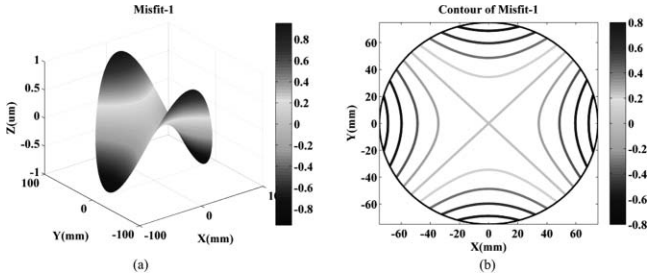

Fig. 10 Misfit-1 of the outermost off-axis segment with a 150 mm tool.

To validate the simulated results, the projection method is adopted. Given the tool size, a projection is performed along the central point's normal direction, and the sag of the local off-axis segment can be obtained. Sag *X* and Sag *Y* defined in the new reference frame established in Sec. 2 can be calculated, as shown in Fig. 12(a). Sag *X*, Sag *Y*, and their difference are all plotted in Fig. 12(b). The difference between Sag *X* and Sag *Y* with PV of 1.96 μm is approximately equal to Misfit-1 with PV of 1.91 μm. This confirms the simulation results.

6 Relevance to a Grolishing Tool

We consider the representative case of a 50 mm diameter hard grolishing tool, mounted on a standard 80 mm radius-of-curvature Zeeko bonnet. This has been characterized with a raster tool-path and C9 (9 μm) aluminium oxide abrasive. Machine parameters were as follows:

- Raster traverse-rate = 500 mm/min.
- Tool rotation speed = 150 rpm.
- Bonnet inflation pressure = 0.2 bar.

The resulting depth of removal on Zerodur was 4.5 μm, and the volumetric removal rate 3.62 mm^3/min. The tool-wear was determined by measuring a fiducial mark on the active surface of the tool before and after grolishing, using a form Talysurf stylus profilometer. This gave a wear-rate of 15.8 μm /h.

For the raster along the radial direction of the parent asphere (Fig. 8), the time for one raster trajectory is ~2.5 min, and so the tool-wear would be ~0.660 μm. This may be compared with Misfit 2 of 20 nm.

7 Application to Subaperture Interferometry

There are interesting analogies between subaperture interferometry of segments and subaperture polishing or grolishing. Subaperture interferometry is attractive for certain measurement tasks, such as edge-profiles at process stages where local slopes are beyond full-aperture interferometry. The practical diameter of the subaperture is ultimately limited by the misfit between the ideal local aspheric surface and the reference wavefront generated by the interferometer. Local defects are superimposed on this base mismatch. In the absence of null-optics, the effective reference is spherical, rather than the rotationally-symmetric asphere of a grolishing tool. Therefore, if the tool form is defined as a best-fit sphere to the local aspheric surface, the level of misfit can be used to evaluate the difficulty and feasibility of subaperture interferometry. On this condition, misfit in subaperture interferometry for aspheric surface can be also simulated with the method instituted in this paper. Considering using subaperture interferometry up to 250 mm diameter to test the ELT segment surface, the misfit can be computed, which is shown in Fig. 13.

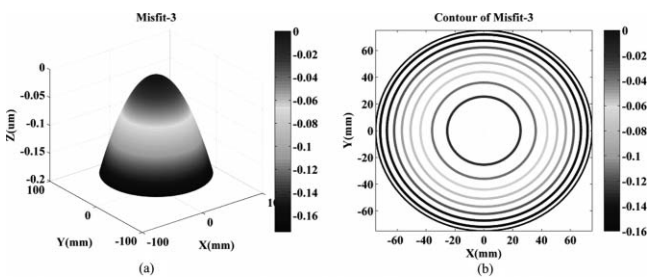

Fig. 11 Misfit-3 of the outermost off-axis segment with a 150 mm tool and 10 mm step-size.

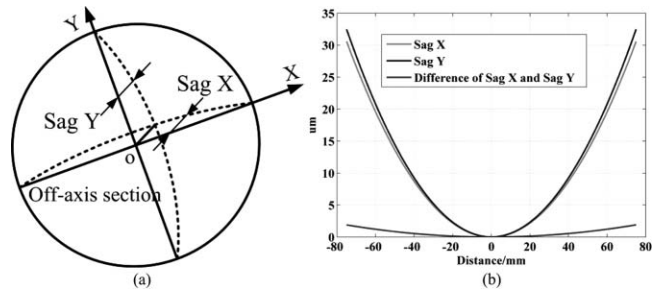

Fig. 12 Rough calculation of the outermost off-axis prototype segment. (a) Definition of Sag *X* and Sag *Y*; (b) Calculation of the difference between Sag *X* and Sag *Y*.

8 Discussions

In this paper, we have examined the quantitative sources of misfit of a rigid tool on an off-axis asphere, including tool-rotation. By separating the sources of misfit, the method presented may be used directly to assess the viability of rotating and nonrotating hard tools, used for different aspheric-segments in a family, at different process-stages, and with different sizes of abrasives. This gives a powerful technique for

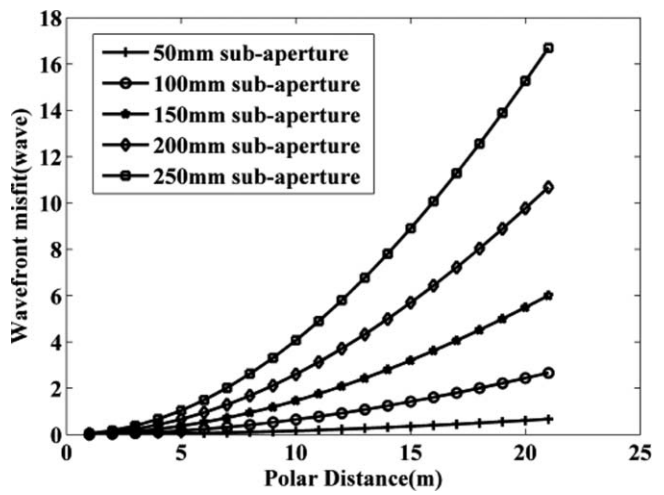

Fig. 13 Wavefront misfit for different measurement subapertures at various polar distances from axis of 42 m primary mirror.

smoothing mid-spatial frequency residuals originating from grinding and subaperture polishing techniques, providing the misfit is properly managed. The method is also relevant to assessing the limits of rotating a non-Newtonian polishing tool[9] to increase removal rate, as such tools adapt to the slow change in asphericity along a tool-path, but behave like hard tools at higher response-frequencies.

Tool Misfit 1, corresponding to the rotational symmetry of the tool mating against a nonrotational surface, is the dominant misfit with rotating hard tools. Of course, this misfit cannot be accommodated by tool-wear. In managing the misfit at different process stages, its magnitude may usefully be compared with i. the abrasive size, and ii. the depth of material to be removed. In this regard, C9 aluminum oxide lapping abrasive can be effectively used with hard tooling up to at least 100 mm diameter, as abrasive size $\gg$ misfit. This provides a useful process-step to smooth mid-spatials on segments following hard-grinding operations.

A somewhat counter-intuitive result related to Misfit 2 is that grolishing tool-paths with C9 abrasive are serviceable that do not correspond to contours of constant asphericity (specifically, to the arcuate trajectories centered on the axis of symmetry of the parent asphere). Even a raster trajectory parallel to the radial direction on the parent asphere is practical, as the change in misfit along the trajectory is less than 1/30 of the corresponding tool-wear. The stepping Misfit 3 is negligible for plausible stepping distances.

Finally, application of the results to calculate the misfit with subaperture interferomtery is such that null optics are not required for realistic subaperture dimensions.

Acknowledgments

Funded by the Chinese Scholarship Council (CSC), the first author conducted this research at the National Facility for Ultraprecision Surface, St. Asaph, United Kingdom, as a visiting scholar of University College London (UCL). In addition, the research is also supported by the Fund of Innovation, Graduate School of NUDT Grant No. B090302, and Hunan Provincial Innovation Foundation for Postgraduate Grant No. CX2009B004. David Walker and Guoyu Yu acknowledge support from the UK Science and Technology Research Council and the UK Engineering and Physical Sciences Research Council.

References

1. ESO the European ELT, "The European Extremely Large Telescope project," (2009), http://www.eso.org/sci/facilities/eelt/.
2. E-ESO-SPE-300–0150 Issue 1, Specifications for the call for tenders "supply of 7 prototype segments of the 42 m diameter E-ELT primary mirror at a firm fixed price of €5.000.000."
3. D. D. Walker, A. Baldwin, R. Evans, R. Freeman, S. Hamidi, P. Shore, X. Tonnellier, S. Wei, C. Williams, and G. Yu, "A quantitative comparison of three grolishing techniques for the Precessions process," *Proc. SPIE Optical Manufacturing and Testing Conference VII*, San Diego, CA, pp. 66711H-1 – H-9 (2007).
4. D. D. Walker, R. Freeman, R. Morton, G. McCavana, and A. Beaucamp, "Use of the 'Precessions'^{TM} process for prepolishing and correcting 2D & $2\frac{1}{2}$D form," *Opt. Express* **14**, 11787–11795 (2006).
5. D. Walker, D. Brooks, A. King, R. Freeman, R. Morton, G. McCavana, and S.-W. Kim, "The 'Precessions' tooling for polishing and figuring flat, spherical and aspheric surfaces," *Opt. Express* **11**, 958–964 (2003).
6. Z. Yang and Li Xin-nan, "Algorithm for the measurement of the parameters of off-axis conic surface," *Astronomical Research and Technology* **5**(3), 307–311 (2008).
7. O. Cardona-Nunez, A. Cornejo-Rodriguez, R. Diaz-Uribe, A. Cordero-Davila, and Jesus Pedraza-Contreras, "Conic that best fits an off-axis conic section," *Appl. Opt.* **25**, 3585–3588 (1986).
8. J. H. Burge, B. Anderson, S. Benjamin, M. K. Cho, K. Z. Smith, and M. J. Valente, "Development of optimal grinding and polishing tools for aspheric surfaces," *Proc. SPIE*, **4451**, 153–164 (2001).
9. D. W. Kim and J. H. Burge, "Rigid conformal polishing tool using non-linear visco-elastic effect," *Opt. Express* **18**, 2242–2257 (2010).

Ci Song is a graduate student specializing in mechanical engineering and is now a PhD candidate and working at the Laboratory of Precision Engineering, Department of Mechatronical Engineering, National University of Defense Technology. His research interests include advanced optical fabrication, aspherical surface fabrication and metrology, magnetorheological finishing (mrf), as well as computer controlled optical surfacing techniques.

David Walker is a professor of optics at University of Wales at Glyndŵr University, and a Professorial Research Associate at University College London. His research lies in computer controlled polishing and measurement, and he co-founded the CNC polishing machine company Zeeko Ltd. in 2000. He currently leads R&D on a project to manufacture seven prototype mirror segments for the 42 m European extremely large telescope.

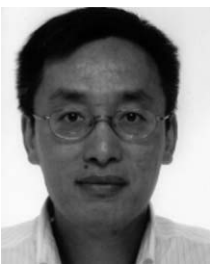

Guoyu Yu is a University of Wales senior research fellow at Glyndwr University. He received his PhD in photonics from Aston University. His past research interests were in the area of fiber Bragg grating, optical semiconductor device modeling, and optical backplane. His current research work is on processing of large aperture aspheric optical surfaces for European extremely large telescope.